Heliyon 10 (2024) e40250

Contents lists available at ScienceDirect

Heliyon

journal homepage: www.cell.com/heliyon

Research article

Energetic and exergoeconomic evaluation of a stig cycle and cooled inlet air gas turbine powered by mixtures of natural gas and H_2 in tropical climates

Juan Fajardo Cuadro [a,*], Deibys Barreto [a], Daniel Yabrudy [a], Andrés Piña-Martinez [c], Oscar Pupo [b], Ana Buelvas [b]

[a] EOLITO Research Unit, Faculty of Engineering, Universidad Tecnológica de Bolívar, Colombia
[b] UREMA Research Unit, Department of Mechanical Engineering, Universidad del Norte, Colombia
[c] ENSIC Research Unit, Université de Lorraine, Nancy, France

ARTICLE INFO

Keywords:
Hydrogen
Natural gas
Gas turbine
Advanced exergy analysis

ABSTRACT

Using pure hydrogen (H_2) or mixtures of H_2 and natural gas in gas-fired power plants represents a viable route to decarbonize electric power generation. This study models a system designed to cool the air at the compressor inlet to 8.8 °C, achieve a flue gas oxygen percentage of 11.46 %, and produce 44.4 MW with a fuel mix ranging from 0 to 100 % H_2 operating in tropical climates, where temperatures exceed 30 °C and relative humidity exceeds 80 %. The analysis is based on energy, exergy, and exergoeconomic balance to obtain performance indicators that characterize plant operations. The results show that with 100 % H_2, the PCI increases by 144 % compared to 100 % natural gas. Furthermore, the energy analysis indicates that for every 10 % volume increase in the H_2 fuel mix, the CO_2 concentration decreased by 34 kg/m^3, the NOx concentration increased by 1 kg/m^3, the dew point temperature increased by 0.5 °C, the energy efficiency improved by 4.5 percentage points, the heat rate decreased by 7 %, and the specific fuel consumption decreased by 8.5 %. Furthermore, the total exergy destruction increased by 14.83 %, and the total exergy efficiency decreased by 2.7 percentage points. The exergoeconomic analysis shows that the specific cost of electric energy per GJ decreases by 10 % for H_2 contents higher than 80 % by volume. This work demonstrates that generating energy from gas turbine power plants with lower CO_2 equivalent emissions is possible. On the other hand, the effects of moisture content in exhaust gases and NO_X are known due to the greater presence of H_2 and higher temperature combustion.

1. Introduction

According to IEA 2023 [1], global energy consumption continues to increase due to technological advances, population growth, and industrialization. Currently, natural gas, coal, and oil contribute around 80 % of the world's energy requirements, which increases greenhouse gases (GHG) [2]. This increasing demand highlights the necessity to investigate additional renewable energy sources to

* Corresponding author.
E-mail addresses: jfajardo@utb.edu.co (J. Fajardo Cuadro), dbarreto@utb.edu.co (D. Barreto), dyabrudy@utb.edu.co (D. Yabrudy), andres-david.pina-martinez@univ-lorraine.fr (A. Piña-Martinez), opupo@uninorte.edu.co (O. Pupo), buelvasana@uninorte.edu.co (A. Buelvas).

https://doi.org/10.1016/j.heliyon.2024.e40250
Received 17 July 2024; Received in revised form 22 October 2024; Accepted 7 November 2024
Available online 9 November 2024

reduce the environmental effects of fossil fuels and address climate change [3]. To achieve this, the power sector must be decarbonized entirely by mid-century. Approximately two-thirds of GHG emissions stem from energy production and use, making transitioning from fossil fuels to power generation crucial for reducing emissions [4]. Hydrogen has emerged as a promising energy carrier that could play a critical role in decarbonizing difficult-to-reduce sectors, such as peak electricity production, industrial heating, and transportation [5]. Blending hydrogen and natural gas in gas-fired power plants could be a viable strategy for decarbonizing the electricity sector. This method utilizes existing infrastructure and has the potential to significantly reduce carbon emissions. However, the effectiveness and practicality of this solution remain uncertain and require further research and development to fully assess its impact and feasibility in the transition to sustainable energy systems. Different authors have used various methodologies to study the performance of gas turbines fed with natural gas and H_2 mixtures. Gaeta A. et al. [6] used dynamic mathematical models coupled with operating conditions such as mechanical power, H_2 fraction ambient temperature, and electrical machine efficiency. Meziane S. and Betebbiche A [7] conducted a numerical study of gas-H_2 fuel mixtures in a micro gas turbine's RQL combustion chamber. Marin G.E. et al. [8] simulated the installation and operation of a thermal power plant gas turbine with an H_2 fuel production system. The fuel used was a mixture of 5 % H_2 and 95 % natural gas, and they concluded that few modifications are required in the gas turbine design.

On the other hand, in the study developed by Oberg et al. [9], they suggest that the use of the turbine is more competitive in the operation of the combined cycle because it is capable of operating with 100 % H2. Likewise, they conclude that in wind generation systems, the gas turbine with H2 works better than in solar systems because there are fewer fluctuations during the generation of electric energy, so it has a longer duration.

The research conducted by Banihabib R. et al. [10] demonstrated that in a hydrogen gas turbine operating on 100 % hydrogen, only 62 PPM was produced under standard conditions, which included 15 % reference oxygen in the exhaust gas. However, the authors did not address the economic implications of using hydrogen as fuel in their study.

Furthermore, numerical simulations conducted by Tamang and Park [11] indicate that mixing propane with hydrogen in a combustion chamber leads to an increase in flame temperature while simultaneously reducing CO and CO_2 emissions. These findings align with results from the study by Benaissa et al. [12]. However, the analysis does not address how the rise in flame temperature affects nitrous oxide (NOx) emissions.

Pashchenko [13] analyzes a combined cycle power plant operating with different amounts of fuel mixture and H_2 to analyze the influence of H_2 content on carbon dioxide emissions and the energy efficiency of the process. Where H_2 was obtained from two processes: 1) methane dilution and 2) steam methane reforming. When hydrogen obtained by methane dilution is used, a decrease in carbon dioxide emissions is observed. In this case, H_2-rich fuel with 20, 50, and 75 % by volume reduces CO_2 emissions by 7.2, 23.5, and 51.1 %, respectively. This data underscores the potential of hydrogen content to significantly reduce CO_2 emissions, offering hope for the future of energy efficiency. Similarly, when hydrogen is used from steam methane reforming, a substantial reduction in CO_2 emissions of 27 % is observed when methane is completely reformed.

The results of the studies by Olaniyi O. et al. [14] show a reduction in carbon emissions and an increase in energy efficiency when using hydrogen fuel to generate energy. In turn, NOx emissions increased along with a 16 % increase in the volumetric flow of the fuel when the hydrogen content was 20 %. The authors also observed that the mixture of hydrogen and natural gas influences the levelized cost of the fuel. Finally, the main advantage from an economic point of view when using hydrogen as fuel depends mainly on its price difference from that of natural gas. These findings open up avenues for further research and exploration in the field of hydrogen fuel.

Regarding the use of gas turbines for the generation of energy through mixtures of natural gas and hydrogen, Incer-Valverde et al. [15] economically evaluate a cogeneration plant to regasify liquid hydrogen. Their process, consisting of two central systems: Open cycle gas turbine and Closed cycle gas turbine with helium, underscores the importance of your role in furthering this research. They conclude that the expander is the component that represents the highest cost of the equipment, followed by the turbomachinery and the cryogenic H_2 regasified. For their part, Skabelund et al. [16] conclude that incorporating H_2 influences the performance of a process, the emissions, and the combustion kinetics of a simulated plant that uses a gas turbine.

Koc Y. et al. [17] evaluated the energy production and the thermal and exergy efficiencies of simple cycles and heat recovery cycles operating with gas turbines that produce 50 MW at 450 °C. The fuel used in both cycles consists of natural gas and hydrogen. The results suggest that the heat recovery cycle is more efficient than the simple cycle at 18 bar using both natural gas and hydrogen. On the other hand, the efficiency of the simple cycle is higher than that of the heat recovery cycle at pressures higher than 18 bar because the compressor outlet temperature is higher than the turbine outlet temperature. The authors conclude that in terms of execution, environmental impact, and CO_2 emissions, gas turbine cycles with H_2 perform better than natural gas, offering a promising solution for reducing carbon emissions. In turn, hydrogen and natural gas costs were 0.345 $/kWh and 0.075 $/kWh, respectively at 20 bar. At 4 bar, the simple cycle costs were $0.322/kWh and $0.071/kWh.

In this study, we use various mixtures of hydrogen (H_2) and natural gas as fuels to analyze their effects on CO_2 and NOx emissions, gas temperature, and energy variables, including conventional and advanced exergetic. The electric power production is set at 44,448 kW with a 3 % oxygen content in the exhaust gases for all the evaluated mixtures.

This paper is structured into four sections. The first section offers background information and outlines the scope of the work. Section 2 details the configuration of the gas power stig cycle and air cooling and the methodology used, including the thermodynamic model, energy analysis, exergy analysis and exergoeconomic analysis by Mixtures of Natural Gas and H_2. Section 3 discusses the research findings and key results from energy analysis, exergy analysis and exergoeconomic analysis. The final section presents conclusions and recommendations for future research. Understanding the influence of H_2 and natural gas mixtures on the works of gas turbine power generation systems is crucial for implementing these fuels in the decarbonization process of electrical energy generation. The importance of this work lies in showing the economic, energy, and environmental effects of using hydrogen and natural gas blends in gas turbine and STIG cycle generation plants in tropical climates with high temperatures and high relative humidity.

2. Materials and methods

This section describes the electrical energy generation system, which utilizes Steam-injected gas turbine (Stig) cycles and incorporates air cooling at the compressor inlet. It also includes energy, exergy, and exergoeconomic analyses. The Stig cycle utilizes high-temperature exhaust gases to produce high-pressure steam, which is then injected into the gas turbine's combustion chamber. This cycle offers a straightforward and effective method for enhancing efficiency and increasing power output, particularly for mid-sized plants with power ranges between 1 and 50 MW. Under certain conditions, the performance of the Stig cycle can surpass that of combined cycles, yielding higher specific work and improved efficiency [18].

The air-cooled Stig cycle gas turbine system is shown in Fig. 1. The system comprises a General Electric LM5000 series gas turbine generator, a two-stage pressurized heat recovery steam generator (HRSG), and an air-cooling system comprising two compression refrigeration machines (CH1 and CH2). These machines are configured in series for the evaporators and in parallel for the condensers, allowing the air-cooling temperature to be 8.8 °C. This is the operating condition of the plant studied in this work. The weather conditions reach an average temperature of 32 °C and 80 % relative humidity in the geographical location of the generation plant [13].

Fig. 2 shows the flow chart for carrying out the exergoeconomic analysis of the power generation plant in this study. This diagram shows the stages of the calculations developed from each plant component's mass and energy balances.

2.1. Properties of the natural gas and H_2 fuel mix

The fuel's principal properties are the mixture's molecular weight of the mixture, the lower heating value, the higher heating value, the Wobbe index, and the specific gravity of the mixture. The molecular weight, the lower heating value, and the higher heating value are calculated using Equation (1), Equation (2), and Equation (3), respectively [19].

$$MW_{mix} = \sum fv_i * MW_i \tag{1}$$

$$LHV_{mix} = \sum fv_i * LHV_i \tag{2}$$

$$HHV_{mix} = \sum fv_i * HHV_i \tag{3}$$

Where fv_i, MW_i, HHV_i and LHV_i represents volumetric fractions, molecular weight, higher heating value, and lower heating value of the fuel mixture, respectively.

Besides, Equation (4) and Equation (5) calculate the specific gravity of the mixture and the Wobbe index, respectively. Where MW_{air} corresponds to the molecular weight of air.

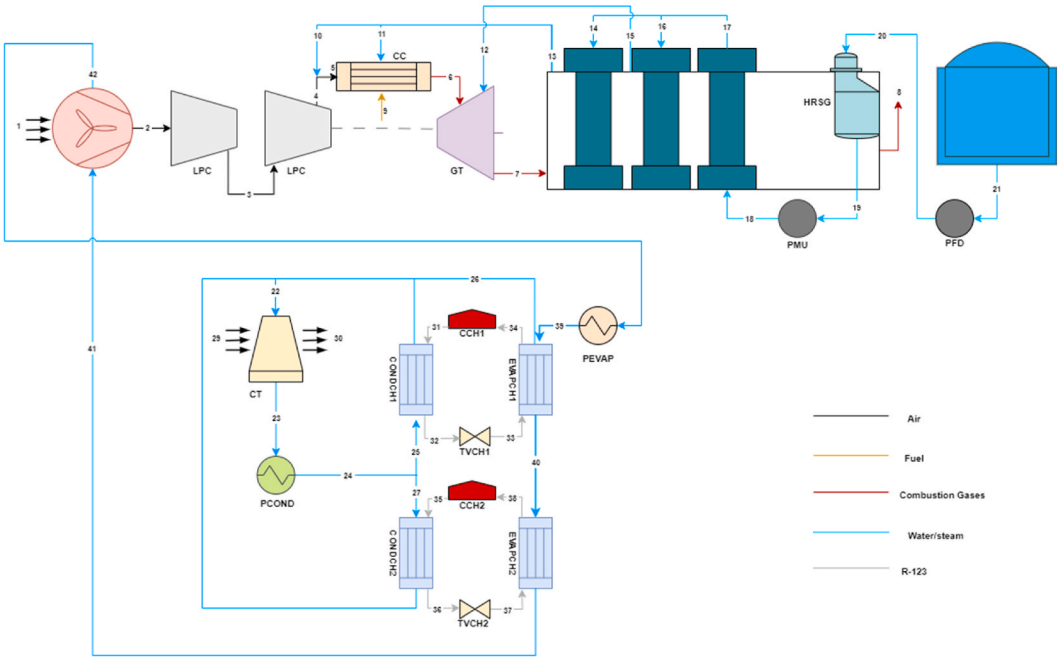

Fig. 1. Diagram of a gas turbine with a Stig cycle and air cooling with a compression refrigeration system.

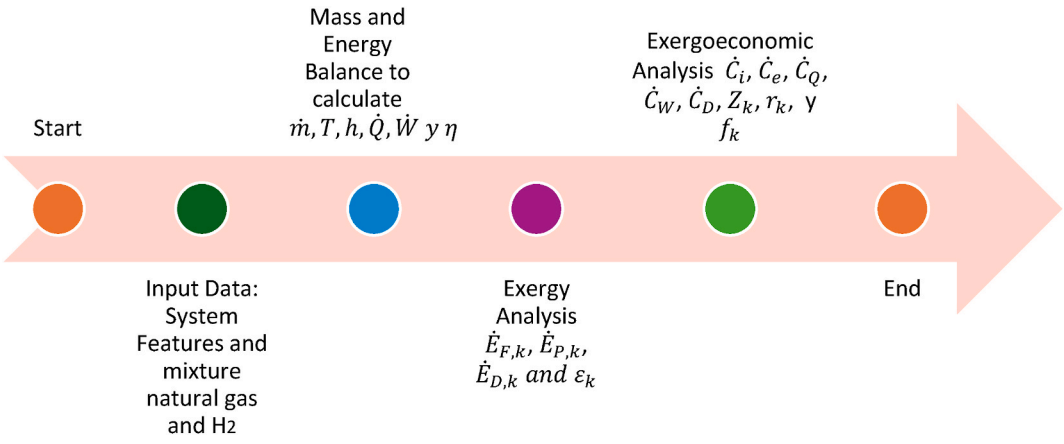

Fig. 2. Flowchart for the exergoeconomic analysis of a gas power cycle using mixtures of hydrogen and natural gas with the Stig cycle and air cooling.

$$SG_{mix} = \frac{MW_{mix}}{MW_{air}} \tag{4}$$

$$W_0 = \frac{HHV}{\sqrt{SG}} \tag{5}$$

2.2. Combustion analysis

The combustion equation for fuel with humid air (Equation (6)) and the enthalpy calculation for this fuel (Equation (7)) are shown below:

$$\left(fvi_{GN}C_xH_y + fvi_{H_2}H_2\right) + \lambda\alpha(O_2 + 3,76N_2) + (\lambda\alpha\underline{\omega} + n_{NO_x})H_2O \rightarrow aCO_2 + bCO + cH_2O + dO_2 + eN_2 + fNO \tag{6}$$

$$H_{Fuel} = fvi_{GN}H_{C_xH_y} + fvi_{H_2}H_{H_2} \tag{7}$$

Where C_xH_y, fvi_{GN}, fvi_{H_2} represents the mixture of GN, and the volumetrics fractions of GN and H_2, respectively. Besides, a, b, c, d, e, and f represent the moles of CO_2, CO, O_2, N_2, and NO present in the exhaust gases. Additionally, the chemical equilibrium equations for dissociation are represented by Equations (8) and (9):

$$CO_2 \rightarrow \frac{1}{2}O_2 + CO \tag{8}$$

$$\frac{1}{2}N_2 + \frac{1}{2}O_2 \rightarrow NO \tag{9}$$

Moreover, Equations (10) and (11) shows the gravimetric humidity and moles of NOx vapor, respectively.

$$\overline{\omega} = 1.608\omega \quad \left(\frac{Mol_{H_2O}}{Mol_{Air}}\right) \tag{10}$$

$$n_{NO_x} = \frac{\dot{m}_{NO_x}MW_{fuel}}{\dot{m}_{fuel}MW_{H_2O}} \quad \left(\frac{Mol_{H_2O}}{Mol_{CH_4}}\right) \tag{11}$$

Where ω, $\dot{m}_{NO_x}$, $\dot{m}_{fuel}$, MW_{fuel} and MW_{H_2O} represents specific air humidity, mass flow of NOx, mixed fuel mass flow, mixed fuel molecular weight, and molecular weight of the humidity. Then, the balance of C, H, O, and N are represented by equations (12)–(15):

$$Balance\ of\ C\ fvi_{GN}x \rightarrow a + b \tag{12}$$

$$Balance\ of\ H\ \left(fvi_{GN}y + 2fvi_{H_2}\right) + 2(\lambda\alpha\underline{\omega} + n_{NO_x}) \rightarrow 2c \tag{13}$$

$$Balance\ of\ O\ 2\alpha\lambda + (\alpha\lambda\underline{\omega} + n_{NO_x}) \rightarrow 2a + b + c + 2d + f \tag{14}$$

$$Balance\ of\ N\ 2\alpha\lambda(3.76) \rightarrow 2e + f \tag{15}$$

Equations (16) and (17) show the equilibrium constants for the ideal gas mixture, while equations (18) and (19) represent the simultaneous formation equations [19].

$$K_{PCO_2} = \frac{b^{V_{CO}} d^{VO_2}}{a^{CO_2}} \tag{16}$$

$$K_{PNO} = \frac{f^{V_{NO}}}{e^{V_{N_2}} d^{V_{O_2}}} \tag{17}$$

$$ln(K_{PCO}) = \frac{-\Delta Giss^{*}_{CO}(T_{Prod})}{R_u T_{Prod}} \tag{18}$$

$$ln(K_{PNO}) = \frac{-\Delta Giss^{*}_{NO}(T_{Prod})}{R_u T_{Prod}} \tag{19}$$

in the combustion chamber's mass balance analysis, we examine the air-fuel ratio, air-vapor ratio, and exhaust gas mass flow. These values are calculated using Equation (20), Equation (21), and Equation (22), respectively [20].

$$AFR = \frac{\dot{m}_{air}}{\dot{m}_{fuel}} = \frac{\propto \lambda M_{O2} + 3.76 \propto \lambda M_{N2} + \propto \lambda \omega M_{H2O}}{MW_{fuel}} \tag{20}$$

$$SAR = \frac{\dot{m}_{Steam}}{\dot{m}_{dry\ air}} \tag{21}$$

$$\dot{m}_{gases} = \dot{m}_{dry\ air}\left(1 + \omega + \frac{1}{AFR} + SAR(CDP + NO_X)\right)\ (kg/s) \tag{22}$$

Where $\dot{m}_{air}$, $\propto$, λ, M_{N2}, $\dot{m}_{Steam}$, $\dot{m}_{dry\ air}$ represents air mass flow, stoichiometric mole of air, air excess, N_2 molecular weight, steam mass flow, and dry air mass flow, respectively.

2.3. Thermodynamic model and energy analysis

The thermodynamic model we use, based on the work of Barreto et al. [21], is applied under the assumption of steady operation of system components. The energy indicators, derived from the first law of thermodynamics and mass balance, are detailed below. These indicators are instrumental in evaluating the plant's operation and performance, even under the challenging and variable conditions of the real atmosphere.

The electrical power generated by the power plant ($\dot{P}_{elect}$) is calculated by multiplying the generator's efficiency (n_{Gen}) by the net power output ($\dot{W}_{Net}$), as shown in Equation (23). The net power output ($\dot{W}_{Net}$), in turn, is determined by subtracting the work consumed by the compressor from the work produced by the turbine.

$$\dot{P}_{Elect} = n_{Gen} \times (\dot{W}_{Net}) \quad (MW) \tag{23}$$

Then, the energy efficiency (η_{TH}) of a power plant with gas turbines is obtained with Equation (24).

$$\eta_{TH} = \frac{\dot{P}_{elect}}{\dot{m}_{fuel} \times LHV_{fuel}} \times 100 \quad (\%) \tag{24}$$

On the other hand, the amount of thermal energy supplied by the fuel needed to generate 1 kW-hour (kWh) of electrical energy is referred to as the heat rate (HR). This metric also serves as an indicator of the plant's performance and is calculated using equation (25).

$$HR = \frac{3600 \times \dot{m}_{fuel} \times LHV_{fuel}}{\dot{P}_{Elect}} \quad \left(\frac{kJ}{kWh}\right) \tag{25}$$

Additionally, the fuel required to generate 1 kW-hour (kWh) of electrical energy is represented by the specific fuel consumption *(SFC)* calculated using Equation (26).

$$SFC = \frac{3600 \times \dot{m}_{fuel}}{\dot{P}_{Elect}} \quad \left(\frac{kg}{kWh}\right) \tag{26}$$

In the exhaust gasses, the most important pollutants studied are concentrations of CO_2 and NO. These are obtained using Equations (27) and (28), respectively:

$$C_{CO2} = \left(\frac{MW_{CO2}}{V_{Gases}}\right) \times fv_{CO2}\ (g/m^3) \tag{27}$$

$$C_{NO} = \left(\frac{MW_{NO}}{V_{Gases}}\right) \times fv_{NO}\left(g / m^3\right) \tag{28}$$

Where MW_{CO2}, MW_{NO}, V_{Gases}, fv_{CO2}, and fv_{NO} are CO2 molecular weight, NO molecular weight, volume of gases, and volumetrics fractions of NO and CO2, respectively.

2.4. Exergetic analysis

In this section, we determine the parameters for exergy analysis. Exergy represents the maximum work potential obtainable from a specific quantity of energy in a given state. It is defined by Equation (29).

$$e_k = e_k^{PH} + e_k^{CH} \tag{29}$$

Where e_k^{PH} and e_k^{CH} are the specific physical exergy and the chemical exergy, respectively.

The specific exergy is determined from the sum of the specific physical exergy plus the specific chemical exergy. It is important to note that the specific physical exergy of a substance is determined using Equation (30), while the specific physical exergy of a gas mixture is determined from Equation (31). Moreover, $C_{P,k}$ described in Equation (32) represents the specific heat of each gas mixture component.

Table 1
Determination of product exergy and fuel exergy of each component of the power production plant with Stig cycle and air cooling.

Component	Fuel exergy and product exergy definition
CCoil	$\dot{E}_F = \dot{m}_{42}e_{42} - \dot{m}_{41}e_{41}$
	$\dot{E}_P = \dot{m}_1 e_1 - \dot{m}_2 e_2$
LPC	$\dot{E}_F = \dot{W}_{LPC}$
	$\dot{E}_P = \dot{m}_3 e_3 - \dot{m}_2 e_2$
HPC	$\dot{E}_F = \dot{W}_{HPC}$
	$\dot{E}_P = \dot{m}_4 e_4 - \dot{m}_3 e_3$
CC	$\dot{E}_F = \dot{m}_9 e_9$
	$\dot{E}_P = \dot{m}_6 e_6 - \dot{m}_5 e_5 - \dot{m}_{11} e_{11}$
GT	$\dot{E}_F = \dot{m}_6 e_6 + \dot{m}_{12} e_{12} - \dot{m}_7 e_7$
	$\dot{E}_P = \dot{W}_{GT}$
Gen	$\dot{E}_F = \dot{W}_{Net}$
	$\dot{E}_P = \dot{P}_{Elect}$
HRSG	$\dot{E}_F = \dot{m}_7 e_7 - \dot{m}_8 e_8$
	$\dot{E}_P = \dot{m}_{13}e_{13} - \dot{m}_{14}e_{14} + \dot{m}_{15}e_{15} - \dot{m}_{16}e_{16} + \dot{m}_{17}e_{17} - \dot{m}_{18}e_{18} + \dot{m}_{19}e_{19} - \dot{m}_{20}e_{20}$
MUP	$\dot{E}_F = \dot{W}_{MUP}$
	$\dot{E}_P = \dot{m}_{18}e_{18} - \dot{m}_{19}e_{19}$
FDP	$\dot{E}_F = \dot{W}_{FDP}$
	$\dot{E}_P = \dot{m}_{20}e_{20} - \dot{m}_{21}e_{21}$
CT	$\dot{E}_F = \dot{m}_{22}e_{22} - \dot{m}_{23}e_{23}$
	$\dot{E}_P = \dot{m}_{30}h_{30} - \dot{m}_{29}h_{29} + \dot{W}_{fan}$
Pcond	$\dot{E}_F = \dot{W}_{Pcond}$
	$\dot{E}_P = \dot{m}_{24}e_{24} - \dot{m}_{23}e_{23}$
CCh1	$\dot{E}_F = \dot{W}_{CCh1}$
	$\dot{E}_P = \dot{m}_{31}e_{31} - \dot{m}_{34}e_{34}$
CondCh1	$\dot{E}_F = \dot{m}_{31}e_{31} - \dot{m}_{32}e_{32}$
	$\dot{E}_P = \dot{m}_{26}e_{26} - \dot{m}_{25}e_{25}$
TVCH1	$\dot{E}_F = \dot{m}_{32}e_{32}$
	$\dot{E}_P = \dot{m}_{33}e_{33}$
EvapCh1	$\dot{E}_F = \dot{m}_{40}e_{40} - \dot{m}_{39}e_{39}$
	$\dot{E}_P = \dot{m}_{34}e_{34} - \dot{m}_{33}e_{33}$
CCh2	$\dot{E}_F = \dot{W}_{CCh2}$
	$\dot{E}_P = \dot{m}_{35}e_{35} - \dot{m}_{38}e_{38}$
CondCh2	$\dot{E}_F = \dot{m}_{35}e_{35} - \dot{m}_{36}e_{36}$
	$\dot{E}_P = \dot{m}_{28}e_{28} - \dot{m}_{27}e_{27}$
TVCh2	$\dot{E}_F = \dot{m}_{36}e_{36}$
	$\dot{E}_P = \dot{m}_{37}e_{37}$
EvapCh2	$\dot{E}_F = \dot{m}_{41}e_{41} - \dot{m}_{40}e_{40}$
	$\dot{E}_P = \dot{m}_{38}e_{38} - \dot{m}_{37}e_{37}$
Pevap	$\dot{E}_F = \dot{W}_{Pevap}$
	$\dot{E}_P = \dot{m}_{39}e_{39} - \dot{m}_{42}e_{42}$

$$e_k^{PH} = h - h_0 - T_0(s - s_0) \tag{30}$$

$$e_k^{PH} = \frac{1}{M_k}\left(C_{P,k}(T - T_0) - T_0\left[C_{P,k}\, ln\left(\frac{T}{T_0}\right) - Rln\left(\frac{P}{P_0}\right)\right]\right) \tag{31}$$

$$C_{P,k} = \sum fv_i C_{P,i} \tag{32}$$

Where fv_i and $C_{P,i}$ represent volumetric fractions and specific heat value of each component, respectively, then, P, h, s and , T represent pressure, specific enthalpy, specific entropy, and temperature, respectively. Then, h_0, T_0, P_0, and s_0 represent pressure, specific enthalpy, specific entropy, and temperature, of the dead state respectively. Moreover, M_k and R are molecular weight and universal gas constant of each component, respectively.

On the other hand, from Equation (33), it is possible to determine the specific chemical exergy of the gas mixture [22]. In turn, Equation (34) determines the specific chemical exergy of the fuel [23]. The variables MWk, x, and y represent the molecular weight, carbon moles, and hydrogen moles in the fuel mixture.

$$e_k^{CH} = \frac{1}{MW_k}\left(fv_i e_i^{CH} + RT_0 \sum fv_i\, ln(fv_i)\right) \tag{33}$$

$$\frac{e_k^{CH}}{LHV} = \lambda_F = 1.033 + 0.0169\frac{x}{y} - \frac{0.0698}{x} \tag{34}$$

The exergy balance and efficiency are determined using Equations (35) and (36). The variables $\dot{E}_{F,k}$, $\dot{E}_{P,k}$, and $\dot{E}_{D,k}$ represent the fuel exergy, product exergy, and destroyed exergy, respectively. Additionally, Table 1 presents the calculation of fuel and product exergy for each component of the plant.

$$\dot{E}_{D,k} = \dot{E}_{F,k} - \dot{E}_{P,k} \tag{35}$$

$$\varepsilon_k = \frac{\dot{E}_{P,k}}{\dot{E}_{F,k}} \times 100 \ \ (\%) \tag{36}$$

2.5. Exergoeconomic analysis

The variables necessary for the development of the exergoeconomic analysis are determined below. In this context, the cost balance is represented by Equation (37) [24]. The terms $\dot{C}_{P,k}$, $\dot{C}_{F,k}$, and $\dot{Z}_k^{Tot}$ represent the cost of the product, the cost of fuel, and the investment cost rate and are determined by Equations (38)–(40), respectively.

$$\dot{C}_{P,k} = \dot{C}_{F,k} + \dot{Z}_k^{Tot} \ \left(\frac{\$}{s}\right) \tag{37}$$

$$\dot{C}_{P,k} = c_{P,k}\dot{E}_P \ \left(\frac{\$}{s}\right) \tag{38}$$

$$\dot{C}_{F,k} = c_{F,k}\dot{E}_F \ \left(\frac{\$}{s}\right) \tag{39}$$

$$\dot{Z}_k^{Tot} = \dot{Z}_k + Z_k^{SU} \ \left(\frac{\$}{h}\right) \tag{40}$$

Then, $\dot{Z}_k$ and Z_k^{SU} represent the investment cost and supply investment cost, which are calculated by Equations (41) and (42) [24]. The terms PEC_k, i_r, n_y, RTY, φ, and C_{tot}^{su} represent the equipment purchase costs, investment return percentage, labor hours, operation and maintenance cost rate, and raw water or coolant supply costs, respectively. Moreover, $\dot{C}_{P,k}$ and $\dot{C}_{F,k}$ represent cost of product and cost of fuel, respectively. The cost functions used to calculate the PEC_k of plant components are detailed in Table 10.

$$\dot{Z}_k = \frac{PEC_k\left[\frac{i_r(1+i_r)^{n_y}}{(1+i_r)^{n_y}-1}\right]\varphi}{3600(RTY)} \ \left(\frac{\$}{h}\right) \tag{41}$$

$$Z_k^{SU} = \frac{C_{tot}^{su} PEC_k}{3600(RTY)\sum PEC_k}\left(\frac{\$}{h}\right) \tag{42}$$

The other variables considered in developing the exergoeconomic analysis include the cost rate of exergy destruction (Equation (43)), the relative cost difference (Equation (44)), and the exergoeconomic factor (Equation (45)) [1,24,25]. In this context, the relative cost difference indicates the relative increase in cost per unit of exergy between the input and output flows of each component [25]. Meanwhile, the exergoeconomic factor illustrates the contribution of non-exergy costs to the overall increase in total cost [1].

$$\dot{C}_D = c_{F,k}\dot{E}_{D,k}\ (\$/h) \tag{43}$$

$$r_k = \frac{c_{P,k} - c_{F,k}}{c_{F,k}} \times 100 \quad (\%) \tag{44}$$

$$f_k = \frac{\dot{Z}_k}{\dot{Z}_k + \dot{C}_D} \times 100 \quad (\%) \tag{45}$$

Finally, Table 2 shows the cost balances applied to each component together with their auxiliary equations. The auxiliary equations of each component depend on their configuration and are obtained from the equations developed by S.C. Obiora et al. [4].

It is important to note that the Supplementary Material outlines the algorithm developed in EES, which includes all the equations for the energy, exergetic, and exergoeconomic variables used in this study.

3. Results and discussion

In this section, the results of the thermodynamic model applied to the gas turbine power plant with Stig cycle and air cooling at the compressor inlet will be shown and discussed. Subsequently, energy, energy, exergy, and exergoeconomic analyses will be conducted. In this context, the objective of the thermodynamic model developed at EES was to calculate the properties of each of the process streams. The results, as shown in Table 3, confirm the model's successful fit to the output power and energy efficiency parameters, with an error of less than 5 %, instilling confidence in its performance.

Table 2
Exergoeconomic cost balance determination for each plant component and auxiliary equations.

Component	Costs balance and auxiliary equations
CCoil	$\dot{C}_{42} - \dot{C}_{41} = \dot{C}_1 - \dot{C}_2 + \dot{Z}_{CCoil}$
	$c_1 = 0, c_{42} = c_{41}$
LPC	$\dot{C}_3 - \dot{C}_2 = \dot{C}_{\dot{W}_{LPC}} + \dot{Z}_{LPC}$
HPC	$\dot{C}_4 - \dot{C}_3 = \dot{C}_{\dot{W}_{LPC}} + \dot{Z}_{HPC}$
Air humidifier	$\dot{C}_5 = \dot{C}_4 + \dot{C}_{10}$
	$\frac{\dot{C}_5}{\dot{E}_5} = \frac{\dot{C}_4 + \dot{C}_{10}}{\dot{E}_4 + \dot{E}_{10}}$
CC	$\dot{C}_6 - \dot{C}_5 - \dot{C}_{11} = \dot{C}_9 + \dot{Z}_{CC}$
GT	$\dot{C}_{\dot{W}_{GT}} = \dot{C}_6 + \dot{C}_{12} - \dot{C}_7 + \dot{Z}_{GT}$
	$\frac{\dot{C}_7}{\dot{E}_7} = \frac{\dot{C}_6 + \dot{C}_{12}}{\dot{E}_6 + \dot{E}_{12}}$
Gen	$\dot{C}_{P_{Elect}} = \dot{C}_{\dot{W}_{Net}} + \dot{Z}_{Gen}$
HRSG	$\dot{C}_{13} - \dot{C}_{14} + \dot{C}_{15} - \dot{C}_{16} + \dot{C}_{17} - \dot{C}_{18} + \dot{C}_{19} - \dot{C}_{20} = \dot{C}_7 - \dot{C}_8 + \dot{Z}_{HRSG}$
	$\frac{\dot{C}_8}{\dot{E}_8} = \frac{\dot{C}_7}{\dot{E}_7}$
	$c_{14} = c_{16} = c_{17}$
	$\frac{\dot{C}_{13} - \dot{C}_{14}}{\dot{E}_{13} - \dot{E}_{14}} = \frac{\dot{C}_{15} - \dot{C}_{16}}{\dot{E}_{15} - \dot{E}_{16}} = \frac{\dot{C}_{17} - \dot{C}_{18}}{\dot{E}_{17} - \dot{E}_{18}} = \frac{\dot{C}_{19} - \dot{C}_{20}}{\dot{E}_{19} - \dot{E}_{20}}$
MUP	$\dot{C}_{18} - \dot{C}_{19} = \dot{C}_{\dot{W}_{MUP}} + \dot{Z}_{MUP}$
FDP	$\dot{C}_{22} - \dot{C}_{21} = \dot{C}_{\dot{W}_{FDP}} + \dot{Z}_{FDP}$
CT	$\dot{C}_{23} - \dot{C}_{32} = \dot{C}_{30} - \dot{C}_{29} + \dot{C}_{\dot{W}_{Fan}} + \dot{Z}_{CT}$
	$c_{29} = 0$
Pcond	$\dot{C}_{24} - \dot{C}_{23} = \dot{C}_{\dot{W}_{Pcond}} + \dot{Z}_{Pcond}$
	$c_{23} = 0$
CCh1	$\dot{C}_{31} - \dot{C}_{34} = \dot{C}_{\dot{W}_{CCH1}} + \dot{Z}_{CCh1}$
	$c_{34} = 0$
CondCh1	$C_{26} - \dot{C}_{25} = \dot{C}_{31} - \dot{C}_{32} + \dot{Z}_{CondCh1}$
TVCH1	$\dot{C}_{33} = \dot{C}_{32} + \dot{Z}_{TVCh1}$
EvapCh1	$\dot{C}_{34} - \dot{C}_{33} = \dot{C}_{39} - \dot{C}_{40} + \dot{Z}_{EvapCh1}$
	$c_{34} = c_{33}$
CCh2	$\dot{C}_{35} - \dot{C}_{38} = \dot{C}_{\dot{W}_{CCH2}} + \dot{Z}_{CCH2}$
	$c_{38} = 0$
CondCh2	$\dot{C}_{28} - \dot{C}_{27} = \dot{C}_{36} - \dot{C}_{35} + \dot{Z}_{CondCh1}$
TVCh2	$\dot{C}_{37} = \dot{C}_{36} + \dot{Z}_{TVCh2}$
EvapCh2	$\dot{C}_{37} - \dot{C}_{38} = \dot{C}_{41} - \dot{C}_{40} + \dot{Z}_{EvapCh2}$
	$c_{38} = c_{37}$
Pevap	$\dot{C}_{39} - \dot{C}_{42} = \dot{C}_{\dot{W}_{PEvap}} + \dot{Z}_{Pevap}$
	$c_{42} = 0$

3.1. Properties of gas natural and hydrogen mixtures

In relation to assessing fuel properties, Table 4 presents the volumetric composition of the natural gas mixture. Additionally, Table 5 displays the high heating value (HHV), molecular weight (MW), Wobbe index (W_0), and specific gravity (SG) of the mixture of hydrogen and natural gas. Among the analyses, the loss of molecular weight of the mixture is observed, going from 16.4 kg/kmol when the fuel is 100 % natural gas to 2.0 kg/kmol when the fuel is 100 % H_2. When reviewing the effects of increasing H_2 in the mixture, we found that the HHV increases by 50 % of its value compared to that corresponding to 100 % natural gas from H_2 contents greater than 80 %, but when going from 90 to 100 % H_2, the increase in this value is 160 %. Furthermore, the Wobbe index of the fuel mixture remains within the classification limits of natural gas for all H_2 proportions under study [26].

3.2. Combustion analysis results

The environmental analysis results of the combustion products are shown in Table 6, which reports the dew point T_{DP} and the concentration and mass flow of CO_2 and NO_x for the different fuel mixtures. The results indicate that as the H_2 volume fraction rises from 0 % to 100 %, the dew point temperature (T_{DP}) increases by 8.05 °C, while the combustion temperature (T_{comb}) experiences a 5 % increase. NO concentrations increase on average by 0.22 percentage points for every 10 % increase in the proportion of H_2 in the fuel mixture, but the mass flow remains constant for all percentages of H_2. When the volume fraction of natural gas changes from 100 % to 50 %, CO_2 concentration is reduced by 24.89 %. For achieve decarbonization of 50 % the percent H2 in mixture of fuel is around 80 %.

3.3. Energy analysis results

In Table 7, we show the energy analysis results in which we report the mass flows of air and fuel, the heat rate (HR), the specific fuel consumption (SFC) and the thermal efficiency (n_{TH}). We found that by changing the fuel mixture from 100 % Natural Gas to 100 % H_2, the Energy Efficiency reaches a value of 88.1 %, a 50 % heat rate reduction, and a 60 % fuel mass flow reduction. The SFC and the air mass reaches a reduction of 60 % and the air mass 10 %.

3.4. Exergy analysis results

This section discusses the influence of using hydrogen-natural gas mixtures as fuel on the parameters of conventional exergy analysis, focusing on the HRSG, gas turbine, combustion chamber, and compressors.

In Table 8, we report the effects of different fuel mixtures on the combustion chamber's exergy destruction, the destroyed exergy of gas turbine, and the total exergy destruction. The exergy of the fuel mixture increases by 15 % when it goes from 0 to 50 % H_2, and when it reaches 100 % H_2, said value increases by 2.41 times. For every 10 % increase in the H2 volume fraction, the total exergy destruction and the exergy destruction in the combustion chamber decrease by 1.5 % and 2.8 %, respectively. We found that by changing the fuel mixture from 100 % natural Gas to 100 % H_2, the total exergetic efficiency reaches a value of 42.84 %.

3.5. Exergoeconomic analysis results

This section discusses the influence of using hydrogen-natural gas mixtures as fuel on the parameters of exergoeconomic analysis, focusing on the HRSG, gas turbine, combustion chamber, and compressors.

The parameters used in developing the exergoeconomic analysis and the equations used to calculate the PEC of each component are shown in Table 9 and Table 10, respectively. Likewise, the results of the exergy destruction cost for each fuel mixture, the specific exergy cost of the fuel, and the specific cost of the electricity generated are shown in Table 11. With mixtures of up to 50 % H_2, the specific fuel cost increases by 10 %, and with 100 % H_2, the increase is of 30 %. The specific electrical energy cost per GJ decreases by 10 % for H_2 contents greater than 80 %. For H_2 contents greater than 60 %, the cost of destroyed exergy is reduced by 10 %, and with 100 % H_2, the reduction is of 20 %.

As shown in Table 12, the relative cost difference varies less than 10 % with changes from 0 to 100 % in H_2 content. Still, the cooling coil's value increases by approximately six times, and in the combustion chamber, it is reduced by approximately 30 %.

On the other hand, Table 13 shows the results of the lower rate of exergy destruction cost in the cooling coil. These results suggest that using 100 % hydrogen reduces the cost of exergy destruction of all processes by up to 20 %, except for the combustion chamber, where it is reduced by up to 10 %.

Table 14 shows the major exergoeconomic factors present in the cooling coil because it presents the lowest values of the rate of exergy destruction cost and the highest for the different H_2 contents in the cooling coil. Increasing the H_2 content in the fuel from 0 to 100 % increases the exergoeconomic factor by 10 % in the Cooling Coil and the combustion chamber, 20 % in the HRSG, and 30 % in

Table 3
The thermodynamic model validation of the plant.

Stig cycle and air cooling	Real data values	Model values	Error (%)
Output power (kW)	45000	44055	2.1
Energy Efficiency (%)	38	42,1	2,1

Table 4
Volumetric composition of refinery gas.

Compound	Volume fraction (%)
CH_4	97.95 %
C_2H_6	0.25 %
C_3H_8	0.05 %
C_4H_{10}	0.03 %
C_5H_{12}	0.01 %
C_6H_{14}	0.02 %
CO_2	0.21 %
N_2	1.48 %

Table 5
Properties of the natural gas and H_2 fuel mixture.

Natural Gas [%]	H_2 [%]	*MW* $\left[\frac{kg}{kmol}\right]$	*SG* [−]	*HHV* $\left[\frac{kJ}{kg}\right]$	*HHV* $\left[\frac{kJ}{kg}\right]$ Ratio to 0 % H_2	*Wo* $\left[\frac{kJ}{m^3}\right]$
100	0	16.4	0.56	53757	1.00	49242
90	10	14.9	0.52	54946	1.02	48073
80	20	13.5	0.47	56387	1.05	46904
70	30	12.1	0.42	58171	1.08	45744
60	40	10.6	0.37	60438	1.12	44609
50	50	9.2	0.32	63412	1.18	43530
40	60	7.8	0.27	67486	1.26	42557
30	70	6.3	0.22	73410	1.37	41792
20	80	4.9	0.17	82813	1.54	41450
10	90	3.5	0.12	100035	1.86	42081
0	100	2.0	0.07	141764	2.64	45584

Table 6
Combustion analysis results.

H_2 [%]	C_{CO_2} $\left[\frac{g}{m^3}\right]$	C_{NO} $\left[\frac{g}{m^3}\right]$	CO_2 $\left[\frac{Ton}{h}\right]$	CO_2 $\left[\frac{Ton}{h}\right]$ Ratio to 0 % H_2	NO $\left[\frac{Ton}{h}\right]$	NO $\left[\frac{Ton}{h}\right]$ Ratio to 0 % H_2	T_{DP} [°C]	H_2O $\left[\frac{m^3}{h}\right]$	H_2O $\left[\frac{m^3}{h}\right]$ Ratio to 0 % H_2	T_{comb} [°C]	T_{comb} [°C] Ratio to 0 % H_2
0	358.7	118.7	22.4	1.00	7.43	1.00	49.0	30.4	1.00	1258	1.00
10	347.4	118.9	21.7	0.97	7.42	1.00	49.3	30.8	1.01	1260	1.00
20	334.3	119.3	20.8	0.93	7.42	1.00	49.6	31.1	1.02	1262	1.00
30	318.9	119.7	19.8	0.88	7.42	1.00	50.0	31.5	1.04	1265	1.01
40	300.4	120.2	18.5	0.83	7.42	1.00	50.4	32.1	1.05	1268	1.01
50	277.8	120.8	17.1	0.76	7.42	1.00	51.0	32.7	1.07	1271	1.01
60	249.7	121.6	15.2	0.68	7.41	1.00	51.6	33.5	1.10	1276	1.01
70	213.6	122.6	12.9	0.58	7.41	1.00	52.5	34.4	1.13	1282	1.02
80	165.8	123.9	9.9	0.44	7.40	1.00	53.5	35.7	1.17	1289	1.02
90	99.1	125.7	5.8	0.26	7.39	1.00	55.0	37.4	1.23	1301	1.03
100	0	118.7	0.0	0.00	7.39	0.99	57.0	39.8	1.31	1317	1.05

the compressors and the gas turbine.

4. Conclusion

Utilizing mixtures of natural gas and hydrogen as fuel is a vital step toward decarbonization of electrical energy generation by reducing CO_2 emissions as the H_2 fraction increases. Analyzing the energetic, exergetic, and exergoeconomic variables of the plant revealed that increasing the percentage of H_2 in the fuel mixture leads to a higher calorific value. This increase results in reductions in the mass flow of air and fuel, heat rate, and specific fuel consumption. Let's consider reaching a 50 % decarbonization in the study system, for this purpose the fuel mixture to be used was of 20 % natural gas and 80 % H_2, this caused an increase the specific fuel exergy cost 20 %, however the specific cost of electricity generated was reduce by 10 %. Is important these findings highlight the potential of H_2-natural gas mixtures to enhance the efficiency and environmental impact of power generation systems.

- The Wobbe index decreases but remains within the classification limits for natural gas across all studied H_2 proportions.
- CO_2 emissions are reduced; however, NOx emissions, dew point, and combustion gas temperature increase.

Table 7
Energy analysis results.

H_2 [%]	$\dot{m}_{fuel}$ $\left[\frac{kg}{s}\right]$	$\dot{m}_{fuel}$ $\left[\frac{kg}{s}\right]$ Ratio to 0 % H_2	$\dot{m}_{air}$ $\left[\frac{kg}{s}\right]$	$\dot{m}_{air}$ $\left[\frac{kg}{s}\right]$ Ratio to 0 % H_2	η_{TH} [%]	η_{TH} [%] Ratio to 0 % H_2	HR $\left[\frac{BTU}{kWh}\right]$	HR $\left[\frac{BTU}{kWh}\right]$ Ratio to 0 % H_2	$\left[\frac{kg}{kWh}\right]$	SFC $\left[\frac{kg}{kWh}\right]$ Ratio to 0 % H_2
0	2.16	1.0	99.7	1.0	42.1	1.0	8105	1.0	0.18	1.0
10	2.12	1.0	99.3	1.0	42.9	1.0	7962	1.0	0.17	1.0
20	2.06	1.0	98.7	1.0	43.8	1.0	7796	1.0	0.17	1.0
30	2.00	0.9	98.1	1.0	44.9	1.1	7600	0.9	0.16	0.9
40	1.93	0.9	97.3	1.0	46.3	1.1	7369	0.9	0.16	0.9
50	1.84	0.9	96.4	1.0	48.1	1.1	7089	0.9	0.15	0.9
60	1.74	0.8	95.2	1.0	50.6	1.2	6744	0.8	0.14	0.8
70	1.60	0.7	93.8	0.9	54.1	1.3	6308	0.8	0.13	0.7
80	1.42	0.7	91.9	0.9	59.4	1.4	5741	0.7	0.12	0.7
90	1.18	0.5	89.3	0.9	68.6	1.6	4973	0.6	0.10	0.5
100	0.84	0.4	85.6	0.9	88.1	2.1	3872	0.5	0.07	0.4

Table 8
Exergy analysis results.

H_2 [%]	e_F $\left[\frac{kj}{kg}\right]$	e_F $\left[\frac{kj}{kg}\right]$ Ratio to 0 % H_2	$E_{D,CC}$ $[kW]$	$E_{D,GT}$ $[kW]$	$E_{D,Total}$ $[kW]$	ε_{Total} [%]
0	50827	1.00	18673	14194	48917	40.12
10	51758	1.02	18446	14152	48573	40.25
20	52911	1.04	18225	14098	48213	40.37
30	54348	1.07	17985	14036	47816	40.51
40	56180	1.10	17712	13962	47361	40.67
50	58591	1.15	17391	13873	46827	40.86
60	61900	1.22	17001	13763	46186	41.08
70	66717	1.31	16512	13624	45392	41.36
80	74371	1.46	15870	13443	44374	41.72
90	88395	1.74	14978	13200	43013	42.19
100	122390	2.41	13587	12852	41074	42.84

Table 9
Parameters used for developing exergoeconomic analysis.

Item	Value
i_r **(%)**	15 %
n_y **(years)**	20
RTY **(hours)**	7446
φ **(−)**	1.06

- The exergy of the fuel increases by 15 % with 50 % H_2 content and by a factor of 2.41 with 100 % H_2.
- Total exergy destruction, as well as exergy destruction in the gas turbine, and combustion chamber decreases with higher H_2 ratios.
- The specific fuel exergy costs increases, and specific exergy costs of the electrical power generated decrease with higher H_2 ratios, addition rate of exergy destruction cost decreases.
- Cost relative differences decrease, while exergoeconomic factors increase, indicating improved economic performance with higher H_2 content.

That is, the main contributions of this work consist in the analysis of the increase in H_2 content in the fuel mixture under the following parameters:

1 The fuel mixture's physical properties.
2 The gas turbine production plant-specific fuel consumption and Thermal efficiency.
3 Exergy Destruction and Exergy Efficiency of Plant Components.
4 The effect of NO_X, CO_2, and humidity concentrations in the exhaust gases.

Future research should focus on examining the effects of varying cooling temperatures and the steam-to-air ratio in a gas turbine

Table 10
Equations to determine the PEC of each component.

Component	PEC Equation	
CCoil	$PEC_{CCoil} = 4112\left(\frac{m_{Air}(h_{in}-h_{out})}{U_{CCoil}\Delta_{LMTD,CCoil}}\right)^{0.6}$	[24]
LPC *HPC*	$PEC_{C} = \frac{71.1 m_{Air}}{0.9-\eta_{Comp}}\left(\frac{P_{out}}{P_{in}}\right)\ln\left(\frac{P_{out}}{P_{in}}\right)$	[24]
CC	$PEC_{CC} = \left(\frac{46.08 m_{gases}}{0.995-\frac{P_i}{P_e}}\right)\times\left(1+e^{(0.018T_e-26.4)}\right)$	[24]
GT	$PEC_{GT} = \frac{49.34 m_{gases}}{0.92-\eta_{GT}}\ln\left(\frac{P_{in}}{P_{out}}\right)\left(1+e^{0.036T_{in}-54.4}\right)$	[24]
Gen	$PEC_{Gen} = 60\dot{P}_{Elect}^{0.65}$	[27]
HRSG	$PEC_{HRSG} = 6570\left[\left(\frac{Q_{EV}}{\Delta_{LMTD,EV}}\right)^{0.8}+\left(\frac{Q_{HP}}{\Delta_{LMTD,HP}}\right)^{0.8}+\left(\frac{Q_{SP}}{\Delta_{LMTD,LP}}\right)^{0.8}\right]+21276 m_{Steam}+1184.4 m_{gases}$	[24]
CT	$PEC_{CT} = 253226.835\left(\frac{\dot{Q}_C}{3600}\right)\left(-0.6936\ln\left(\frac{T_{cw,1}-T_{cw,o}}{2}-T_{wb,amb}\right)+2.1898\right)$	[28]
Pcond	$PEC_{pump} = 3540\dot{W}_{pump}^{0.71}$	[29]
Cond	$PEC_{Cond} = 1773 m_{Refrigerant}$	[30]
Evap	$PEC_{Evap} = 130\left(\frac{A_{Evap}}{0.093}\right)^{0.78}$	[24]
TV	$PEC_{TV} = 114.5 m_{Refrigerant}$	[30]

Table 11
Exergoeconomic analysis results.

H_2 [%]	c_{Fuel} $\left[\frac{\$}{GJ}\right]$	c_{Fuel} $\left[\frac{\$}{GJ}\right]$ Ratio to 0 % H_2	c_{elect} $\left[\frac{\$}{GJ}\right]$	c_{elect} $\left[\frac{\$}{GJ}\right]$ Ratio to 0 % H_2	$\dot{C}_D$ $\left[\frac{\$}{h}\right]$	$\dot{C}_D$ $\left[\frac{\$}{h}\right]$ Ratio to 0 % H_2
0	16.15	1.0	604.7	1.0	57007	1.0
10	16.35	1.0	602.9	1.0	56916	1.0
20	16.57	1.0	600.5	1.0	56498	1.0
30	16.82	1.0	597.6	1.0	56010	1.0
40	17.11	1.1	594.2	1.0	55429	1.0
50	17.47	1.1	590.0	1.0	54728	1.0
60	17.89	1.1	584.8	1.0	53863	0.9
70	18.41	1.1	578.1	1.0	52767	0.9
80	19.05	1.2	569.1	0.9	51332	0.9
90	19.8	1.2	556.6	0.9	49365	0.9
100	20.43	1.3	537.0	0.9	46437	0.8

Table 12
Relative cost difference by component.

H_2 [%]	Ccoil	LPC	HPC	CC	GT	HRSG
0	9.2	12.7	2.9	20.7	13.7	78.5
10	10.2	12.7	2.9	20.4	13.7	78.7
20	11.6	12.7	2.9	20.2	13.7	79.0
30	13.3	12.7	2.9	19.9	13.7	79.3
40	15.3	12.7	2.9	19.6	13.7	79.7
50	17.9	12.7	2.9	19.2	13.7	80.1
60	21.1	12.7	2.9	18.8	13.7	80.7
70	25.3	12.7	2.9	18.2	13.7	81.5
80	31.2	12.7	2.9	17.6	13.7	82.5
90	39.8	12.7	2.9	16.7	13.6	83.8
100	54.0	12.7	2.9	15.4	13.6	85.9

electric power generation system utilizing the Stig cycle and air cooling, particularly with a natural gas and hydrogen mixture. Besides, the challenge currently being faced is ensuring that the plant is economically viable during its operation with green hydrogen since the production costs of green hydrogen remain high compared to hydrogen produced from fossil fuels.

Table 13
Cost rate of destroyed exergy by component.

H_2 [%]	Ccoil	LPC	HPC	CC	GT	HRSG
0	3.9	2407	2762	1086	26613	17352
10	3.9	2389	2742	1084	26457	17268
20	3.8	2366	2716	1084	26253	17162
30	3.8	2340	2685	1084	26014	17037
40	3.7	2308	2648	1085	25729	16887
50	3.7	2269	2604	1085	25387	16705
60	3.6	2222	2550	1085	24965	16479
70	3.5	2163	2482	1083	24434	16192
80	3.4	2087	2395	1076	23743	15811
90	3.2	1984	2276	1057	22805	15283
100	3.0	1835	2105	999	21432	14486

Table 14
Exergoeconomic factor by component.

H_2 [%]	Ccoil	LPC	HPC	CC	GT	HRSG
0	68.18	0.31	2.98	0.89	1.15	0.39
10	68.34	0.31	3.00	0.91	1.18	0.39
20	68.55	0.31	3.03	0.91	1.19	0.39
30	68.79	0.31	3.06	0.91	1.20	0.40
40	69.09	0.32	3.11	0.91	1.21	0.40
50	69.45	0.32	3.16	0.91	1.23	0.40
60	69.89	0.33	3.22	0.91	1.25	0.41
70	70.46	0.34	3.31	0.91	1.28	0.42
80	71.21	0.35	3.42	0.91	1.31	0.43
90	72.24	0.37	3.59	0.93	1.37	0.44
100	73.79	0.40	3.87	0.98	1.45	0.47

CRediT authorship contribution statement

Juan Fajardo Cuadro: Methodology, Conceptualization. **Deibys Barreto:** Validation, Investigation, Formal analysis, Conceptualization. **Daniel Yabrudy:** Formal analysis. **Andrés Piña-Martinez:** Formal analysis. **Oscar Pupo:** Validation, Formal analysis. **Ana Buelvas:** Writing – review & editing, Writing – original draft, Methodology.

Declaration of competing interest

The authors declare the following financial interests/personal relationships which may be considered as potential competing interests:Juan Fajardo reports financial support was provided by Tecnologica University of Bolivar. If there are other authors, they declare that they have no known competing financial interests or personal relationships that could have appeared to influence the work reported in this paper.

Acknowledgment

We sincerely thank the Alternative Energy Research Group—EOLITO of the Universidad Tecnológica de Bolívar —for supporting our research.

Appendix A. Supplementary data

Supplementary data to this article can be found online at https://doi.org/10.1016/j.heliyon.2024.e40250.

Nomenclature

$\dot{Z}$	Investment cost ($/s)
$\dot{W}$	Work (kW)
T	Temperature (°C)
s	Entropy specific (kJ/kgC)
P	Pressure (kPa)
c	Specific cost per unit of exergy ($/kJ)
$\dot{C}$	Total cost ($/s)

(*continued on next page*)

(*continued*)

e	Exergy specific (kJ/kg)
C_P	Specific heat (kJ/kg°C)
h	Specific Enthalpy (kJ/kg)
$\dot{E}$	Exergy (kJ/s)
$\dot{m}$	Mass flow (kg/s)
Greek Letters	
α	Stoichiometric air
η	Energy Efficiency
φ	Operation and maintenance factor
ω	Humidity
λ	Excess air
ε	Exergy Efficiency
Sub-index	
0	Dead state conditions
f	Fuel
D	Destruction
i	Input
o	Output
p	Product
Abbreviations	
AC	Air Cooler
C	Compresor
CC	Combustion chamber
CDP	Fraction of steam injected into the pre-combustion chamber
CH1	Refrigeration of machine 1
CH2	Refrigeration of machine 2
CT	Cooling tower
Cond	Condenser
FAR	Fuel air- ratio
FWP	Pump Feedwater
GT	Gas Turbine
HP	High pressure
HRSG	Heat recovery boiler
IAC	Air cooling inlet compressor
LP	Low-pressure
MWP	Make-up water pump
NOx	Volumetric fraction of Nitrous oxides
P	Pump
Pevap	Evaporation water pump
Pcond	Condensation water pump
PEC	Equipment purchase price
SAR	Steam air-ratio
TV	Throttle valve

References

[1] IEA, World Energy Outlook 2023, 2023. Https://Www.Iea.Org/Reports/World-Energy-Outlook-2023.

[2] S. Orjuela-Abril, J.P. Rojas-Suárez, J.E. Duarte Forero, Study of performance and emissions in diesel engines operating with biodiesel from soybean oil and water emulsions, Aibi Revista de Investigación, Administración e Ingeniería 9 (2021) 19–29, https://doi.org/10.15649/2346030x.935.

[3] W. Li, M. Nadeem, Decarbonizing progress: exploring the nexus of renewable energy, digital economy, and economic development in South American countries, Heliyon 10 (2024) e33446, https://doi.org/10.1016/j.heliyon.2024.e33446.

[4] S.C. Obiora, O. Bamisile, Y. Hu, D.U. Ozsahin, H. Adun, Assessing the decarbonization of electricity generation in major emitting countries by 2030 and 2050: transition to a high share renewable energy mix, Heliyon 10 (2024) e28770, https://doi.org/10.1016/j.heliyon.2024.e28770.

[5] K. Topolski, E.P. Reznicek, B.C. Erdener, C.W. San Marchi, J.A. Ronevich, L. Fring, K. Simmons, O.J. Guerra Fernandez, B.-M. Hodge, M. Chung, Hydrogen Blending into Natural Gas Pipeline Infrastructure: Review of the State of Technology, n.d. www.nrel.gov/publications.

[6] A. di Gaeta, F. Reale, F. Chiariello, P. Massoli, A dynamic model of a 100 kW micro gas turbine fuelled with natural gas and hydrogen blends and its application in a hybrid energy grid, Energy 129 (2017) 299–320, https://doi.org/10.1016/j.energy.2017.03.173.

[7] S. Meziane, A. Bentebbiche, Numerical study of blended fuel natural gas-hydrogen combustion in rich/quench/lean combustor of a micro gas turbine, Int. J. Hydrogen Energy 44 (2019) 15610–15621, https://doi.org/10.1016/j.ijhydene.2019.04.128.

[8] G.E. Marin, B.M. Osipov, A.V. Titov, A.R. Akhmetshin, Gas turbine operating as part of a thermal power plant with hydrogen storages, Int. J. Hydrogen Energy 48 (2023) 33393–33400, https://doi.org/10.1016/j.ijhydene.2023.05.109.

[9] S. Öberg, M. Odenberger, F. Johnsson, The value of flexible fuel mixing in hydrogen-fueled gas turbines – a techno-economic study, Int. J. Hydrogen Energy 47 (2022) 31684–31702, https://doi.org/10.1016/j.ijhydene.2022.07.075.

[10] R. Banihabib, T. Lingstädt, M. Wersland, P. Kutne, M. Assadi, Development and testing of a 100 kW fuel-flexible micro gas turbine running on 100% hydrogen, Int. J. Hydrogen Energy 49 (2024) 92–111, https://doi.org/10.1016/j.ijhydene.2023.06.317.

[11] S. Tamang, H. Park, Numerical investigation of combustion characteristics for hydrogen mixed fuel in a can-type model of the gas turbine combustor, Int. J. Hydrogen Energy 48 (2023) 11493–11512, https://doi.org/10.1016/j.ijhydene.2022.05.273.

[12] S. Benaissa, B. Adouane, S.M. Ali, S.S. Rashwan, Z. Aouachria, Investigation on combustion characteristics and emissions of biogas/hydrogen blends in gas turbine combustors, Therm. Sci. Eng. Prog. 27 (2022) 101178, https://doi.org/10.1016/j.tsep.2021.101178.

[13] D. Pashchenko, Hydrogen-rich gas as a fuel for the gas turbines: a pathway to lower CO2 emission, Renew. Sustain. Energy Rev. 173 (2023) 113117, https://doi.org/10.1016/j.rser.2022.113117.
[14] O. Olaniyi, J. Incer-Valverde, G. Tsatsaronis, T. Morosuk, Exergetic and economic evaluation of natural gas/hydrogen blends for power generation, Journal of Energy Resources Technology, Transactions of the ASME 145 (2023), https://doi.org/10.1115/1.4056448.
[15] J. Incer-Valverde, Y. Lyu, G. Tsatsaronis, T. Morosuk, Economic evaluation of a large-scale liquid hydrogen regasification system, Gas Science and Engineering 119 (2023) 205150, https://doi.org/10.1016/j.jgsce.2023.205150.
[16] B.B. Skabelund, C.D. Jenkins, E.B. Stechel, R.J. Milcarek, Thermodynamic and emission analysis of a hydrogen/methane fueled gas turbine, Energy Convers. Manag. X 19 (2023) 100394, https://doi.org/10.1016/j.ecmx.2023.100394.
[17] Y. Koç, H. Yağlı, A. Görgülü, A. Koç, Analysing the performance, fuel cost and emission parameters of the 50 MW simple and recuperative gas turbine cycles using natural gas and hydrogen as fuel, Int. J. Hydrogen Energy 45 (2020) 22138–22147, https://doi.org/10.1016/j.ijhydene.2020.05.267.
[18] J.B.W. Kok, E.A. Haselhoff, Thermodynamic analysis of the thermal and exergetic performance of a mixed gas-steam aero derivative gas turbine engine for power generation, Heliyon 9 (2023) e18927, https://doi.org/10.1016/j.heliyon.2023.e18927.
[19] Y. Cengel, M. Boles, M. Kanoglu, Thermodynamics: an Engineering Approach, ninth ed., Mc Graw-Hill, New York, 2019.
[20] H. Athari, S. Soltani, M. Rosen, S. Mahmoudi, T. Morosuk, Comparative exergoeconomic analyses of gas turbine steam injection cycles with and without fogging inlet cooling, Sustainability 7 (2015) 12236–12257, https://doi.org/10.3390/su70912236.
[21] D. Barreto, J. Fajardo, G.C. Caballero, Y.C. Escorcia, Advanced exergy and exergoeconomic analysis of a gas power system with steam injection and air cooling with a compression refrigeration machine, Energy Technol. 9 (2021), https://doi.org/10.1002/ente.202000993.
[22] J. Szargut, Exergy Method: Technical and Ecological Applications, WIT Press, Poland, 2005.
[23] E. Açıkkalp, H. Aras, A. Hepbasli, Advanced exergoeconomic analysis of a trigeneration system using a diesel-gas engine, Appl. Therm. Eng. 67 (2014) 388–395, https://doi.org/10.1016/j.applthermaleng.2014.03.005.
[24] A. Bejan, G. Tsatsaronis, M.J. Moran, Thermal Design and Optimization, WILEY, 1995.
[25] A. Abusoglu, M. Kanoglu, Exergetic and thermoeconomic analyses of diesel engine powered cogeneration: Part 1 – formulations, Appl. Therm. Eng. 29 (2009) 234–241, https://doi.org/10.1016/j.applthermaleng.2008.02.025.
[26] Test Gases-Test Pressures-Appliance Categories, 2003.
[27] I. Dincer, Comprehensive Energy System, Elsevier, Amsterdam, 2018.
[28] A. Alashkar, M. Gadalla, Thermo-economic analysis of an integrated solar power generation system using nanofluids, Appl. Energy 191 (2017) 469–491, https://doi.org/10.1016/j.apenergy.2017.01.084.
[29] A. Baghernejad, M. Yaghoubi, Exergoeconomic analysis and optimization of an integrated solar combined cycle system (ISCCS) using genetic algorithm, Energy Convers. Manag. 52 (2011) 2193–2203, https://doi.org/10.1016/j.enconman.2010.12.019.
[30] M. Morid, M.H. Khoshgoftar Manesh, 6E evaluation of an innovative polygeneration system consisting of gas turbine cycle with CO2 capture, ejector refrigeration cycle, steam Rankine cycle, solar tower and MEDAD unit, Therm. Sci. Eng. Prog. 46 (2023) 102234, https://doi.org/10.1016/j.tsep.2023.102234.